

# Binary black hole spin-orbit resonances: a hint at compact binary formation channels

Simon Stevenson

Collaborators

Ilya Mandel, Christopher Berry, Ben Farr, Will Farr



# Nearly finished . . .

## DISTINGUISHING COMPACT BINARY POPULATION SYNTHESIS MODELS USING GRAVITATIONAL WAVE OBSERVATIONS OF COALESCING BINARY BLACK HOLES

SIMON STEVENSON

School of Physics and Astronomy, University of Birmingham, Edgbaston, Birmingham, B15 2TT and  
School of Physics and Astronomy, Cardiff University, The Parade, Cardiff, CF24 3AA, UK

FRANK OHME AND STEPHEN FAIRHURST

School of Physics and Astronomy, Cardiff University, The Parade, Cardiff, CF24 3AA, UK

(Dated: October 10, 2014)  
*Draft version October 10, 2014*

### ABSTRACT

The coalescence of compact binaries containing neutron stars and black holes is thought to be one of the most promising signals for advanced ground-based gravitational wave interferometers, with the first direct detections expected over the next few years. The (mass) distribution of observable signals, as predicted by population synthesis models, is highly uncertain, and poorly constrained parameters in population synthesis models correspond to poorly constrained astrophysics (such as supernova kick velocities, parameters governing the energetics of the common envelope evolution and the strength of stellar winds) at various stages in the evolution of massive binary stars, the progenitors of binary neutron star and binary black hole systems. We simulate gravitational wave observations from a series of population synthesis models including known selection biases and measurement errors and compare the results to the original catalogue of models using a Bayesian model selection framework. We show that one can begin to rule out some models and thus begin to constrain the unknown astrophysics within the first few years of regular detections.

# Outline

- ▣ Motivation
  - ▣ Binaries and Binary evolution
  - ▣ BH spin (mis)alignment
- ▣ Spin precession and resonances
- ▣ Models and results
- ▣ Conclusions/ Future work

# Modern astrophysical sources

## Type 1a supernovae

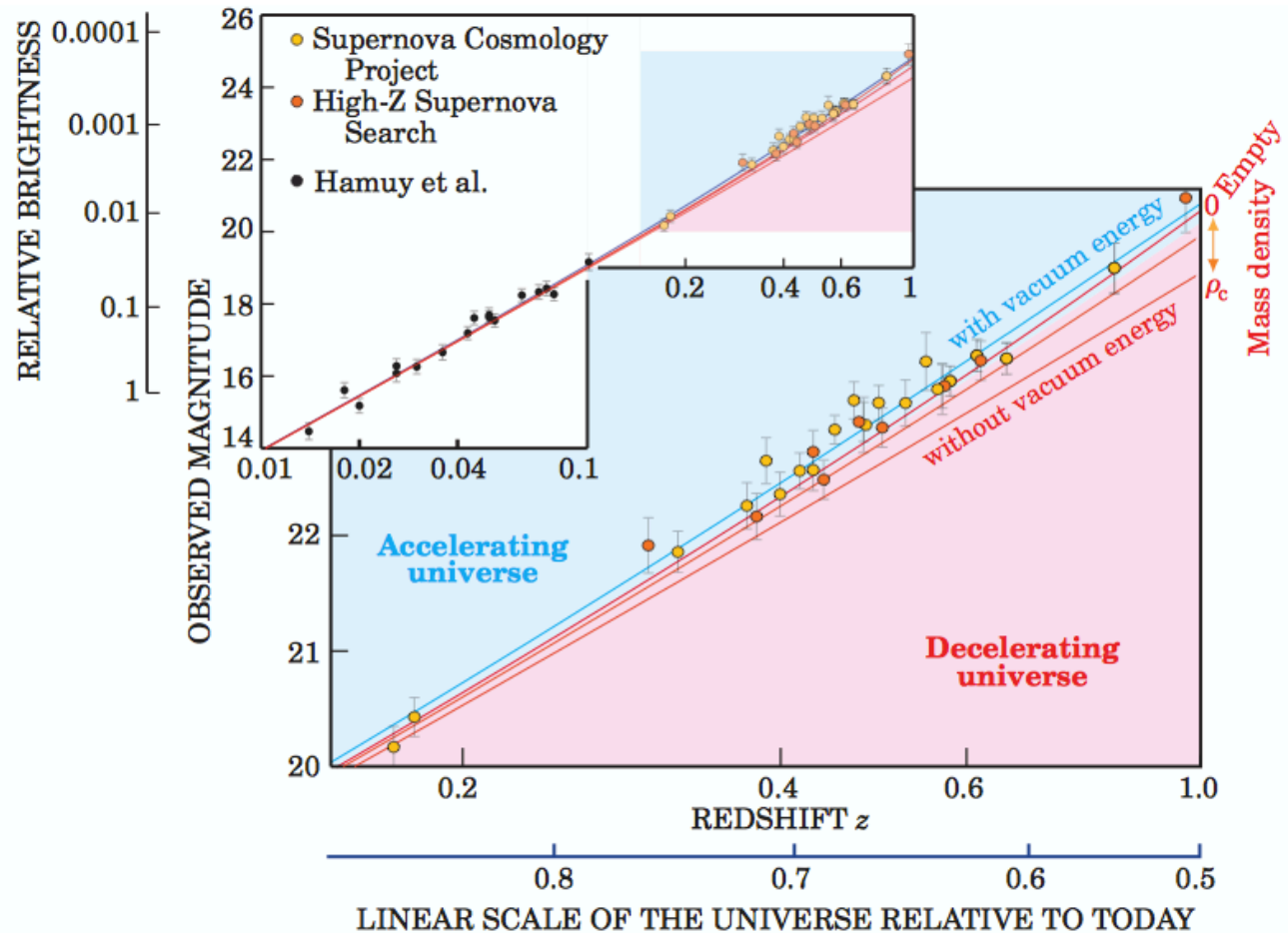


Image credit: <http://www.darkenergysurvey.org/science/SN1A.shtml>

# Modern astrophysical sources

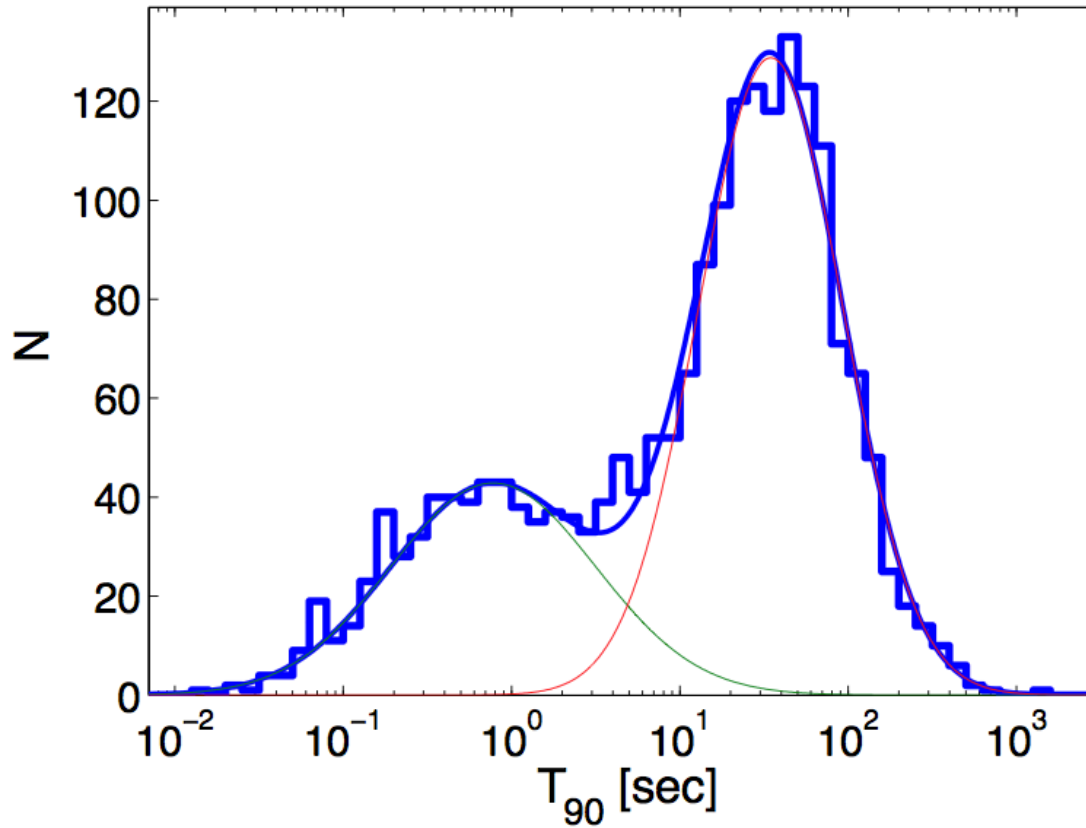
## Type 1a supernovae

**Figure 3. Observed magnitude versus redshift** is plotted for well-measured distant<sup>12,13</sup> and (in the inset) nearby<sup>7</sup> type Ia supernovae. For clarity, measurements at the same redshift are combined. At redshifts beyond  $z = 0.1$  (distances greater than about  $10^9$  light-years), the cosmological predictions (indicated by the curves) begin to diverge, depending on the assumed cosmic densities of mass and vacuum energy. The red curves represent models with zero vacuum energy and mass densities ranging from the critical density  $\rho_c$  down to zero (an empty cosmos). The best fit (blue line) assumes a mass density of about  $\rho_c/3$  plus a vacuum energy density twice that large—implying an accelerating cosmic expansion.



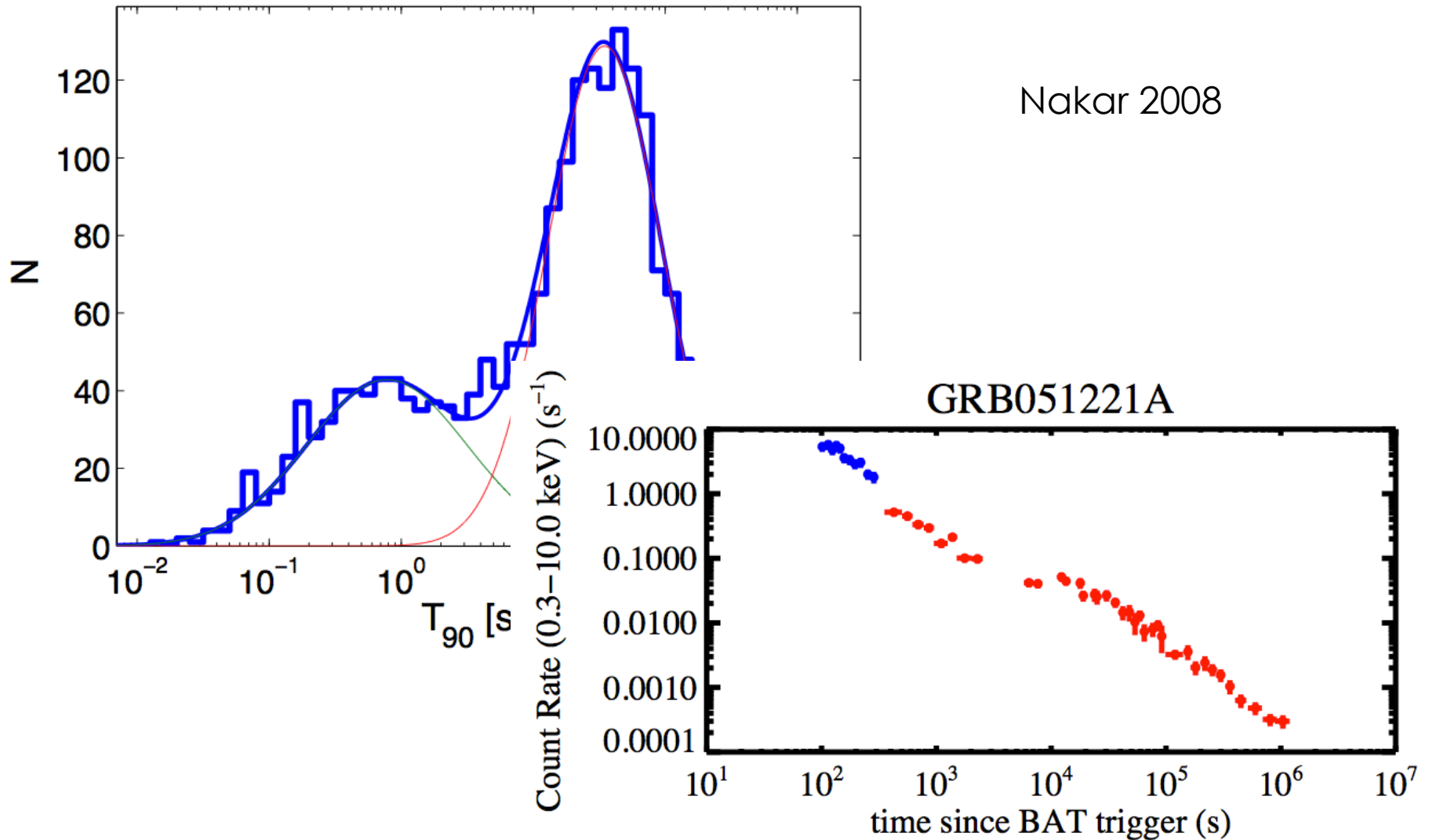
Perlmutter 2003

# Modern astrophysical sources (short) Gamma Ray Bursts (GRBs)



Nakar 2008

# Modern astrophysical sources (short) Gamma Ray Bursts (GRBs)



# Modern astrophysical sources

## Kilonovae

Tanvir et al, *Nature*, 2013

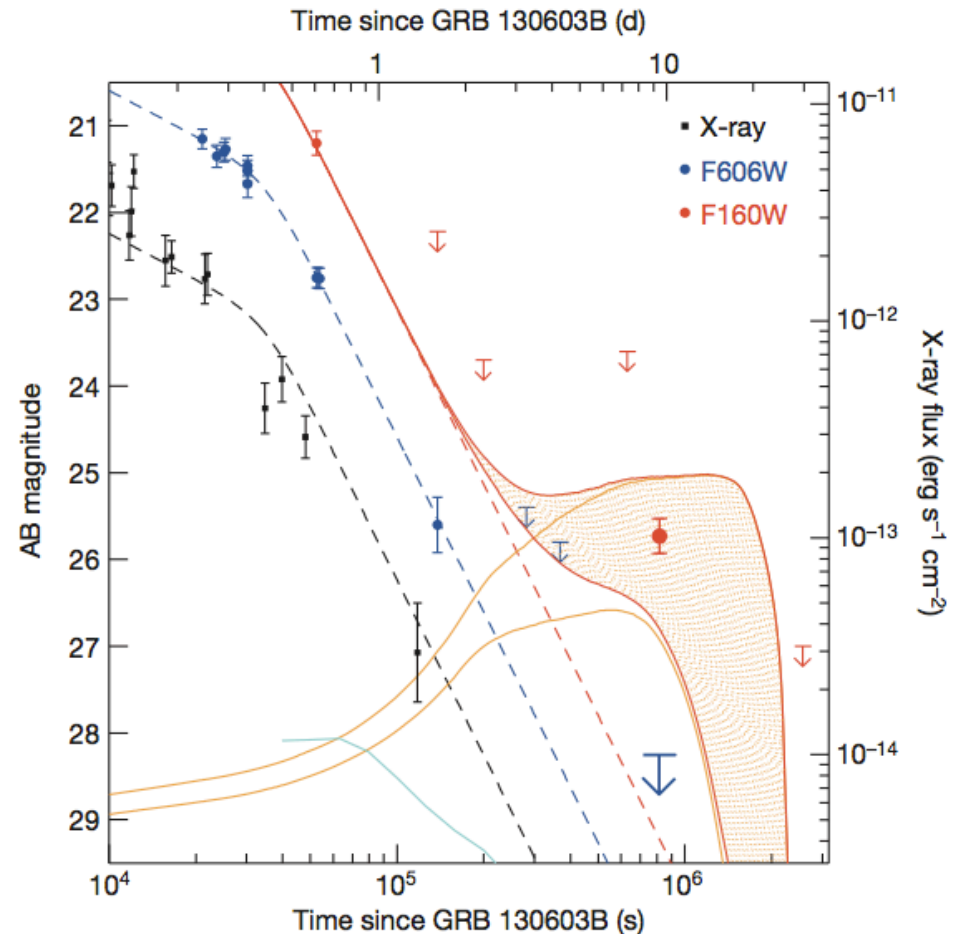
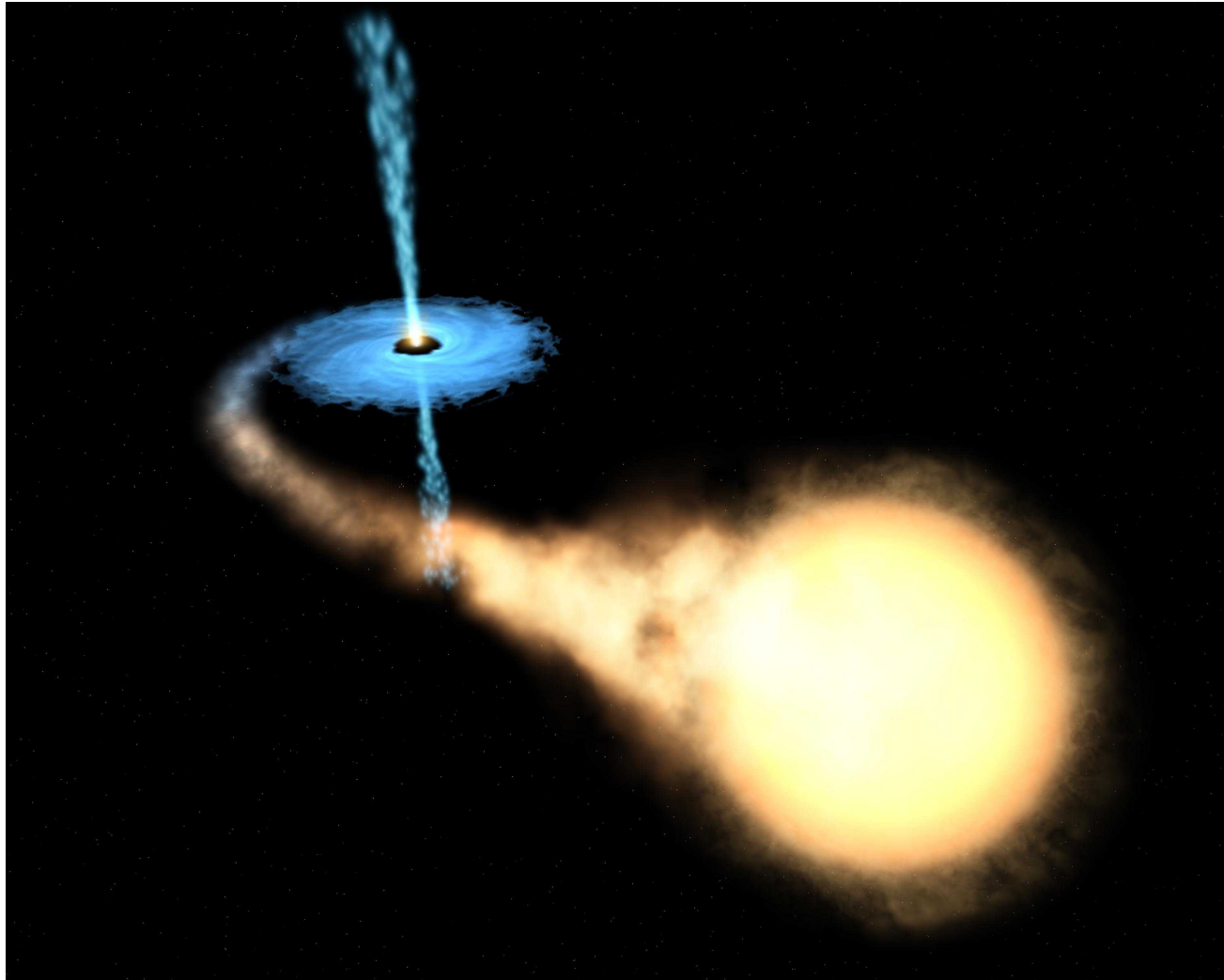


**Figure 2 | Optical, NIR and X-ray light curves of GRB 130603B.** Left axis, optical and NIR; right axis, X-ray. Upper limits are  $2\sigma$  and error bars are  $1\sigma$ . The optical data (g, r and i bands) have been interpolated to the F606W band and the NIR data have been interpolated to the F160W band using an average spectral energy distribution at  $\sim 0.6$  d (Supplementary Information). HST



# Modern astrophysical sources

## X-ray binaries



# Modern astrophysical sources

## Binary and Millisecond Pulsars

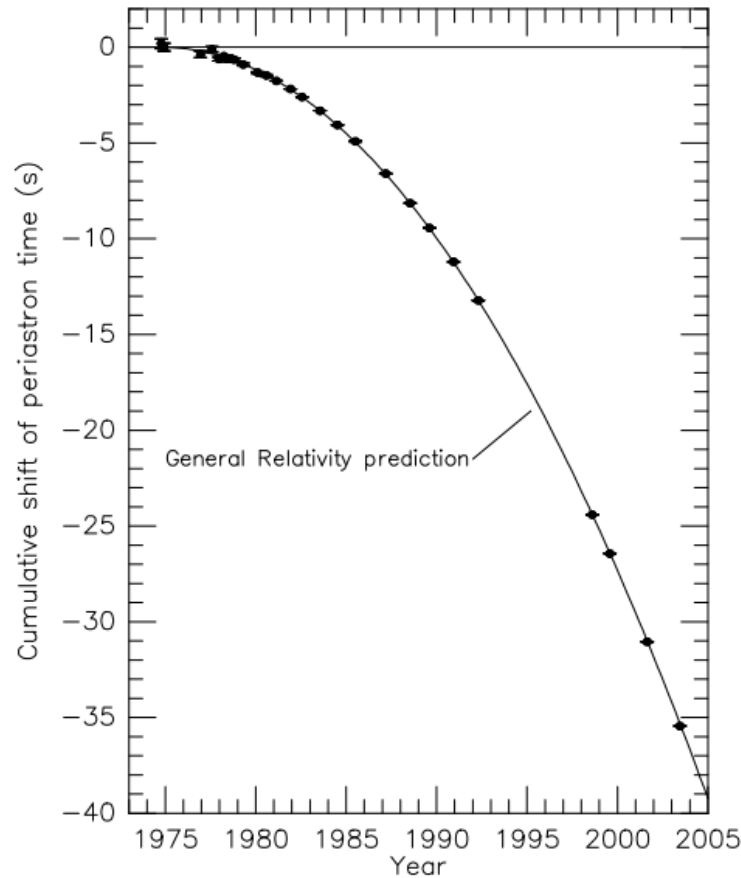


Figure 1. Orbital decay of PSR B1913+16. The data points indicate the observed change in the epoch of periastron with date while the parabola illustrates the theoretically expected change in epoch for a system emitting gravitational radiation, according to general relativity.

Taylor and Weisberg 2005

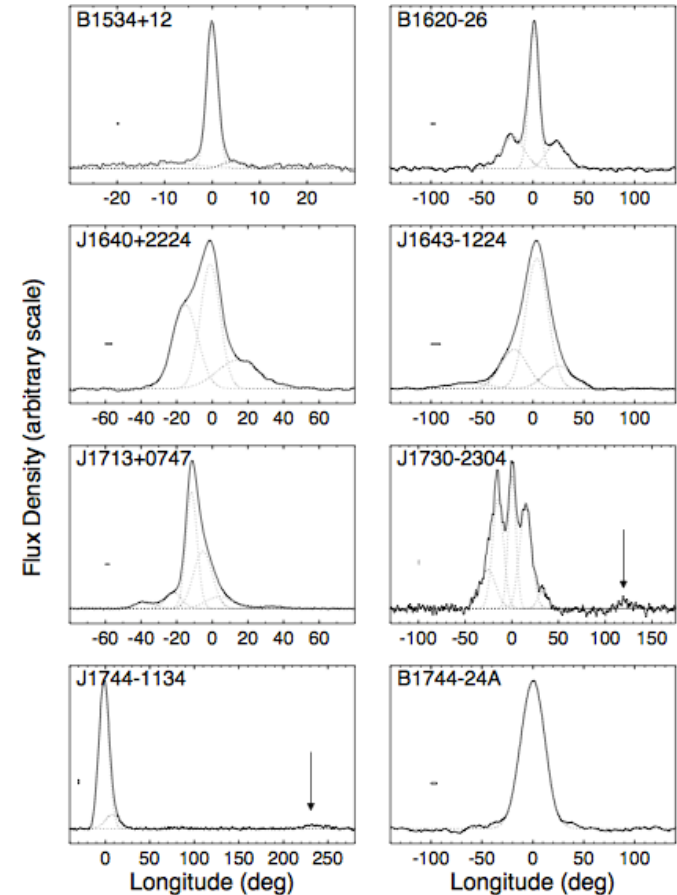


FIG. 6.—Average pulse profiles for eight MSPs at a frequency of 1.4 GHz. The arrows shown for J1730–2304 and J1744–1134 point to a detected postcursor and precursor, respectively.

Kramer et al 1998

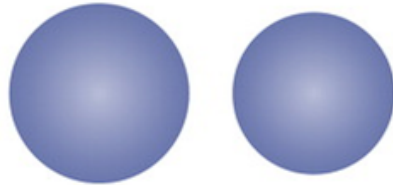
# Modern astrophysical sources

## LIGO sources BNS BBH

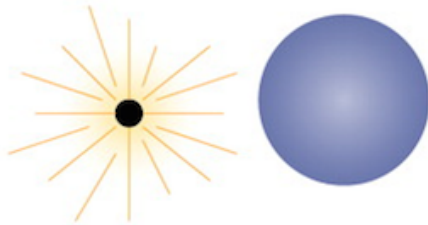


# Binary evolution

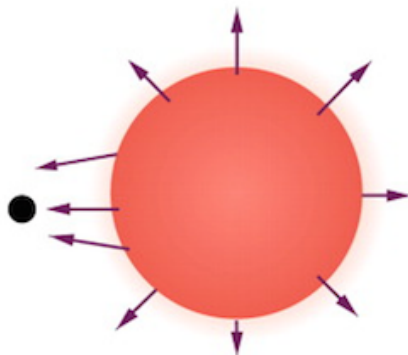
D



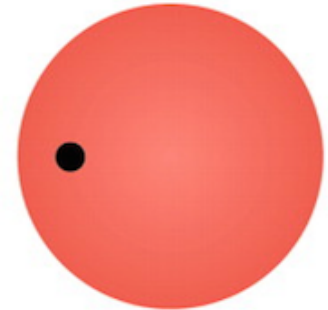
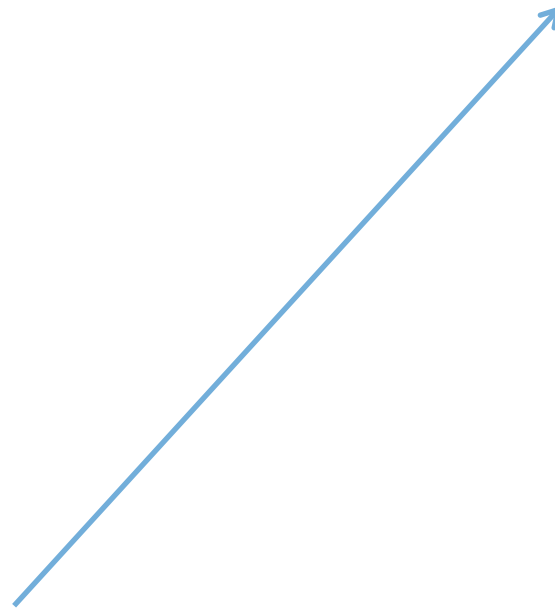
Main-sequence stars, both  $>8 M_{\odot}$



Primary explodes as supernova



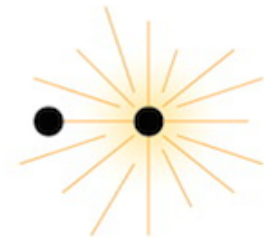
Mass transfer to neutron star  
from companion wind



Common envelope: the NS spirals  
into and expels the envelope of the  
secondary



NS—He-star binary  
Roche-Lobe overflow possible



Secondary explodes as supernova

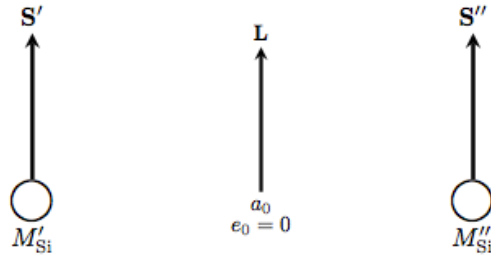


Result: double-neutron-star system  
Example: PSR B1913+16

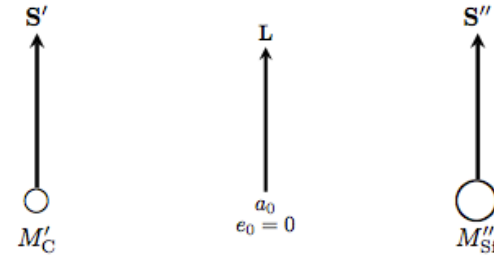
Image + credit <http://www.sciencemag.org/content/304/5670/547/F1.expansion>

# What about spins?

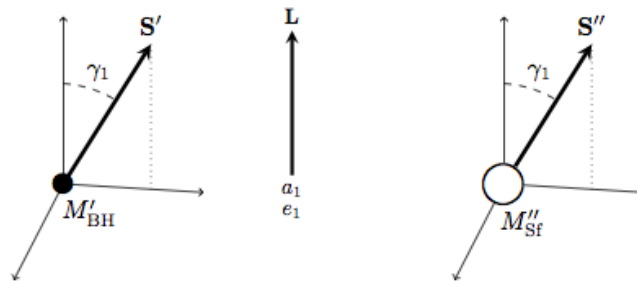
a) Main-sequence binary



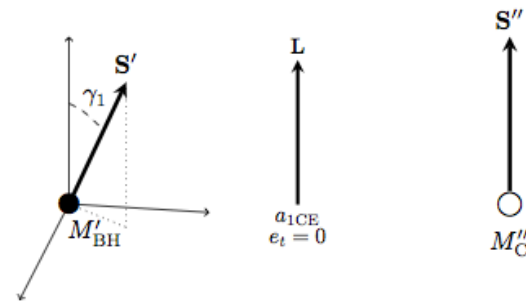
b) First mass-transfer phase



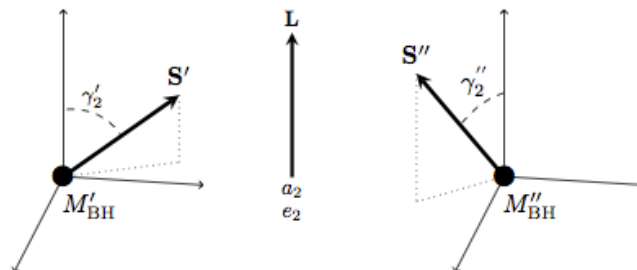
c) 1<sup>st</sup> Supernova explosion



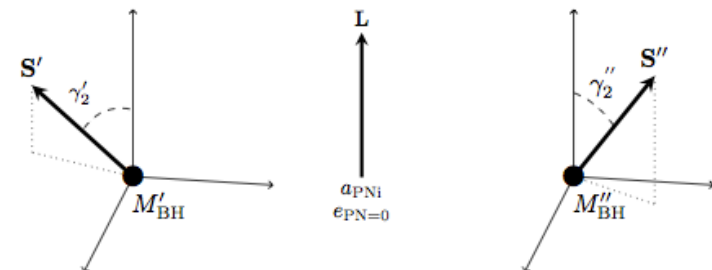
d) Tides, common envelope, BH precession



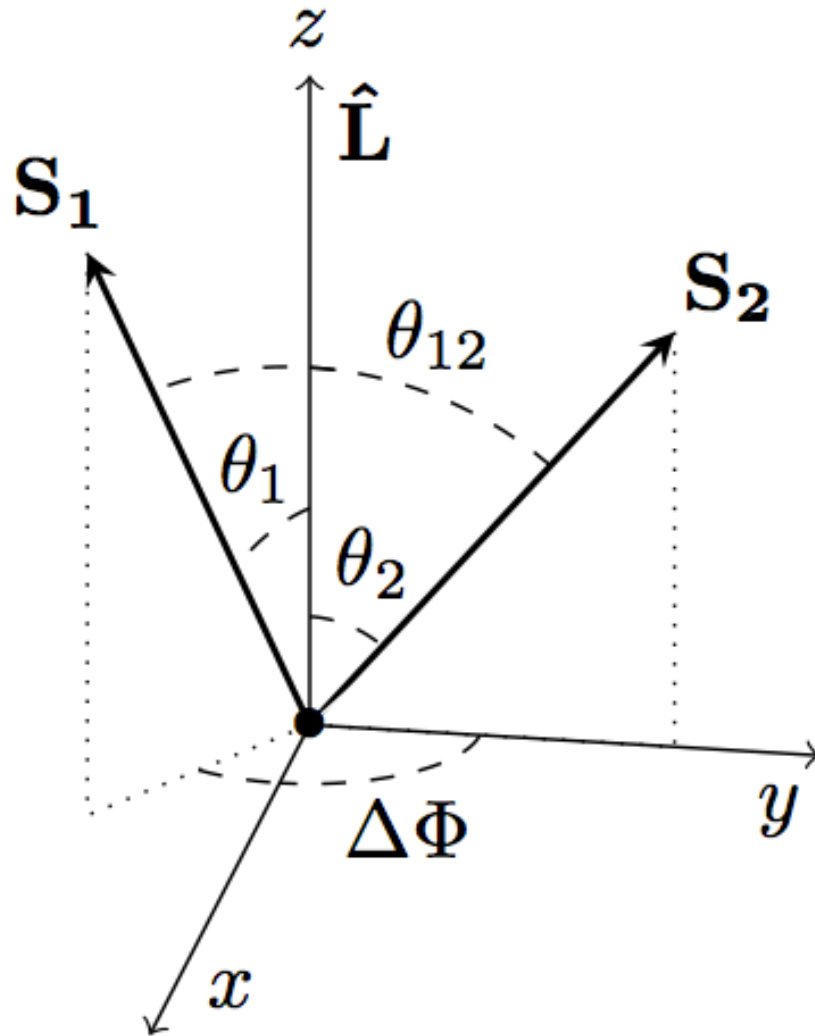
e) 2<sup>nd</sup> Supernova explosion



f) Post-Newtonian evolution



# Frame of reference



$$\cos \theta_1 = \hat{\mathbf{S}}_1 \cdot \hat{\mathbf{L}},$$

$$\cos \theta_2 = \hat{\mathbf{S}}_2 \cdot \hat{\mathbf{L}},$$

$$\cos \theta_{12} = \hat{\mathbf{S}}_1 \cdot \hat{\mathbf{S}}_2.$$

$$\cos \Delta\Phi = \frac{\hat{\mathbf{S}}_1 \times \hat{\mathbf{L}}}{|\hat{\mathbf{S}}_1 \times \hat{\mathbf{L}}|} \cdot \frac{\hat{\mathbf{S}}_2 \times \hat{\mathbf{L}}}{|\hat{\mathbf{S}}_2 \times \hat{\mathbf{L}}|}$$

# Post-Newtonian evolution

$$\frac{d\hat{\mathbf{L}}}{dt} = \frac{-\nu}{\eta M^2} \left[ \frac{d\mathbf{S}_1}{dt} + \frac{d\mathbf{S}_2}{dt} \right]$$

$$\frac{d\mathbf{S}_1}{dt} = \boldsymbol{\Omega}_1 \times \mathbf{S}_1,$$

$$\frac{d\mathbf{S}_2}{dt} = \boldsymbol{\Omega}_2 \times \mathbf{S}_2.$$

$$M\boldsymbol{\Omega}_1 = \eta\nu^5 \left( 2 + \frac{3q}{2} \right) \hat{\mathbf{L}} + \frac{\nu^6}{2M^2} \left[ \mathbf{S}_2 - 3 \left( \hat{\mathbf{L}} \cdot \mathbf{S}_2 \right) \cdot \hat{\mathbf{L}} - 3q \left( \hat{\mathbf{L}} \cdot \mathbf{S}_1 \right) \cdot \hat{\mathbf{L}} \right]$$

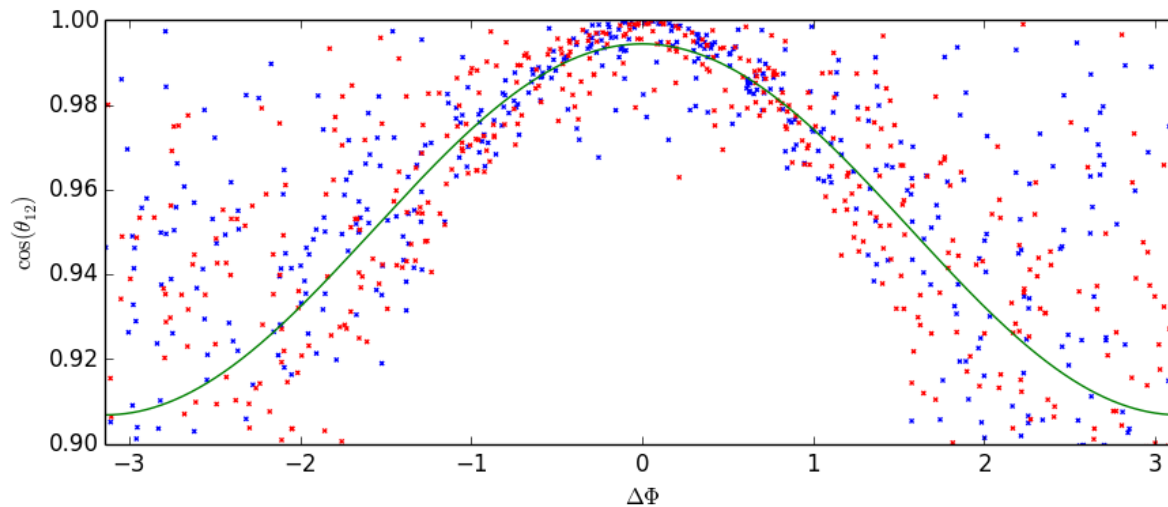
$$M\boldsymbol{\Omega}_2 = \eta\nu^5 \left( 2 + \frac{3}{2q} \right) \hat{\mathbf{L}} + \frac{\nu^6}{2M^2} \left[ \mathbf{S}_1 - 3 \left( \hat{\mathbf{L}} \cdot \mathbf{S}_1 \right) \cdot \hat{\mathbf{L}} - \frac{3}{q} \left( \hat{\mathbf{L}} \cdot \mathbf{S}_2 \right) \cdot \hat{\mathbf{L}} \right]$$

... and

$$\begin{aligned}
 \frac{d\nu}{dt} = & \frac{32}{5} \frac{\eta}{M} \nu^9 \left\{ 1 - \nu^2 \frac{743 + 924\eta}{336} + \nu^3 \left[ 4\pi - \sum_{i=1,2} \chi_i (\hat{\mathbf{S}}_i \cdot \hat{\mathbf{L}}) \left( \frac{113}{12} \frac{m_i^2}{M^2} + \frac{25}{4} \eta \right) \right] \right. \\
 & + \nu^4 \left[ \frac{34103}{18144} + \frac{13661}{2016} \eta + \frac{59}{18} \eta^2 + \frac{\eta \chi_1 \chi_2}{48} \left( 721 (\hat{\mathbf{S}}_1 \cdot \hat{\mathbf{L}}) (\hat{\mathbf{S}}_2 \cdot \hat{\mathbf{L}}) - 247 (\hat{\mathbf{S}}_1 \cdot \hat{\mathbf{S}}_2) \right) \right. \\
 & \left. \left. + \frac{1}{96} \sum_{i=1,2} \left( \frac{m_i \chi_i}{M} \right)^2 \left( 719 (\hat{\mathbf{S}}_i \cdot \hat{\mathbf{L}})^2 - 233 \right) \right] - \nu^5 \pi \frac{4159 + 15876\eta}{672} \right. \\
 & + \nu^6 \left[ \frac{16447322263}{139708800} + \frac{16}{3} \pi^2 - \frac{1712}{105} (\gamma_E + \ln 4\nu) + \left( \frac{451}{48} \pi^2 - \frac{56198689}{217728} \right) \eta + \frac{541}{896} \eta^2 - \frac{5605}{2592} \eta^3 \right] \\
 & \left. + \nu^7 \pi \left[ \frac{-4415}{4032} + \frac{358675}{6048} \eta + \frac{91495}{1512} \eta^2 \right] + \mathcal{O}(\nu^8) \right\}, \quad (43)
 \end{aligned}$$

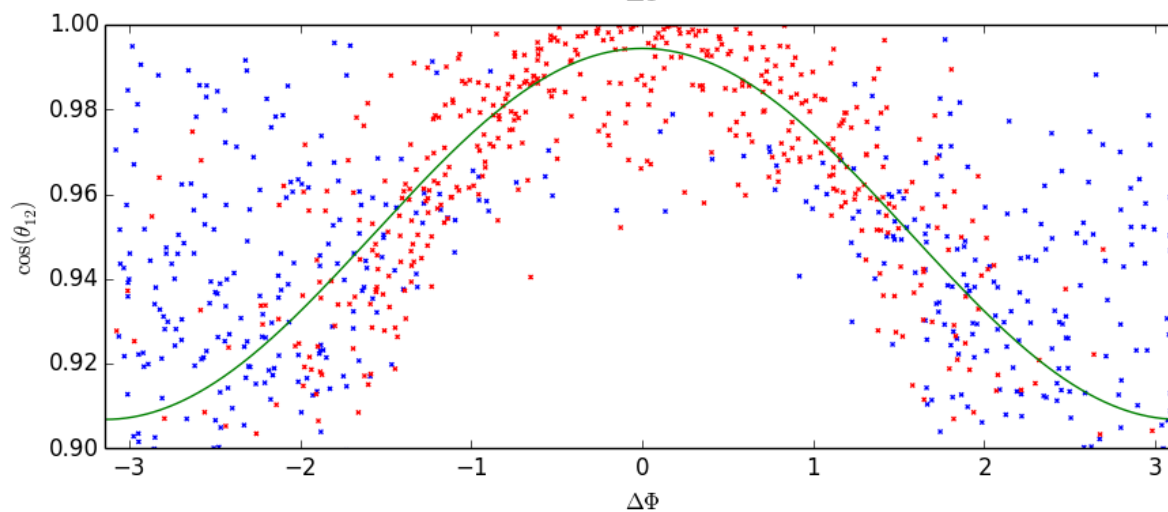


# Spin-orbit resonances



Initially:

$$\theta_1 > \theta_2$$

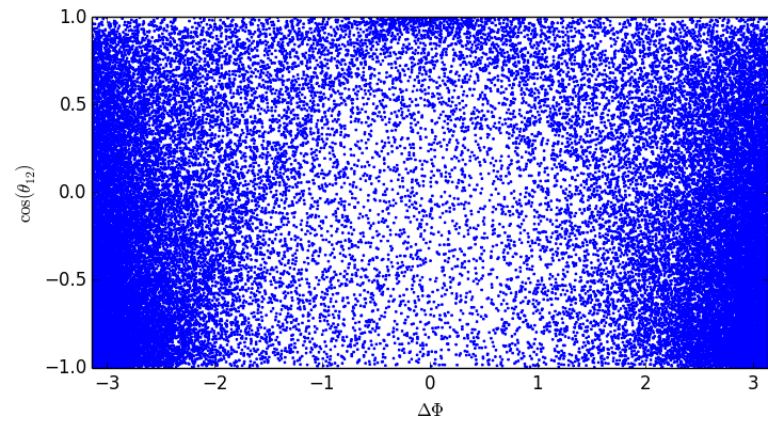
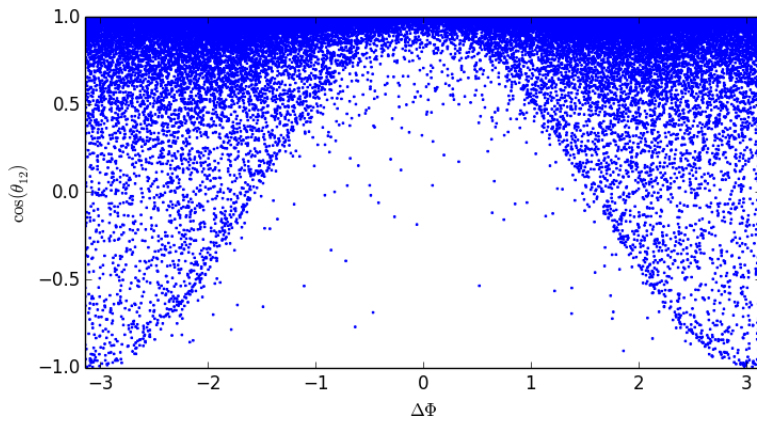
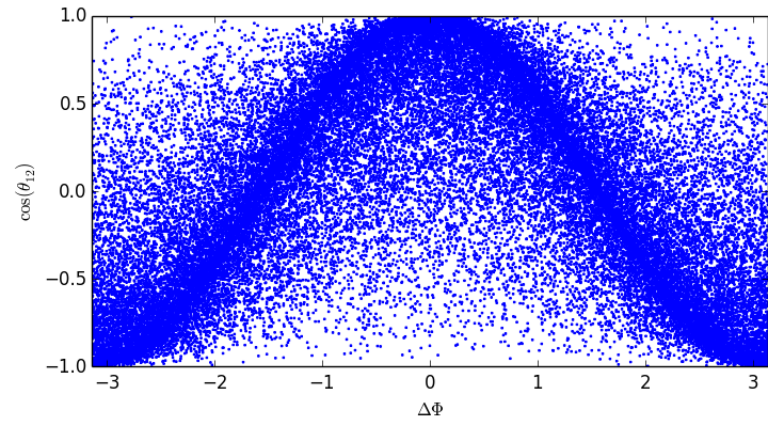
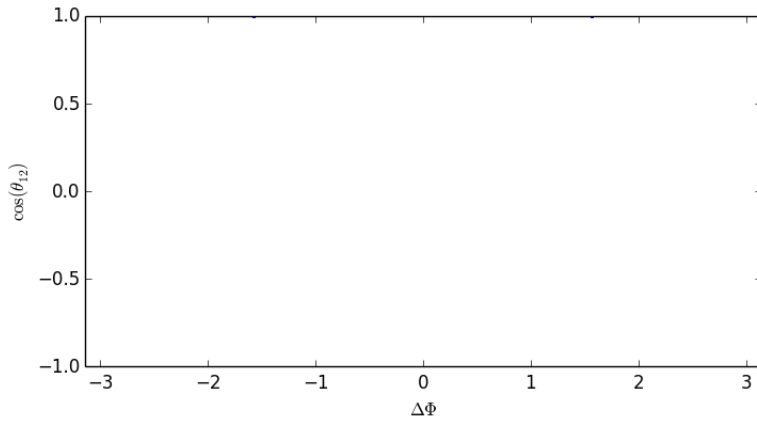


$$\theta_1 < \theta_2$$

# Models for black hole spin misalignment

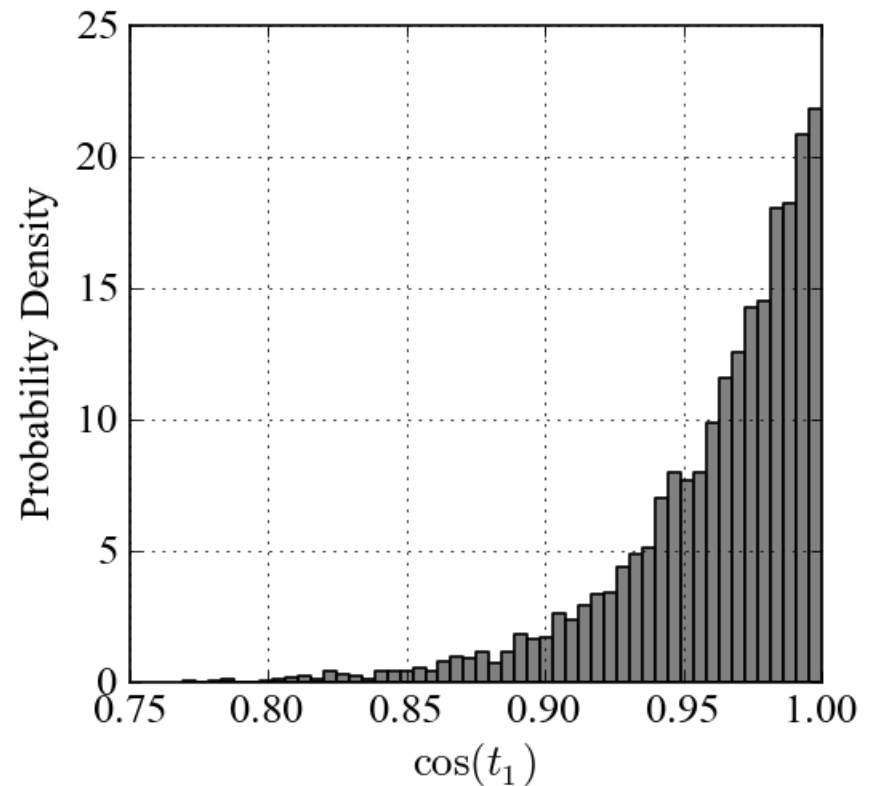
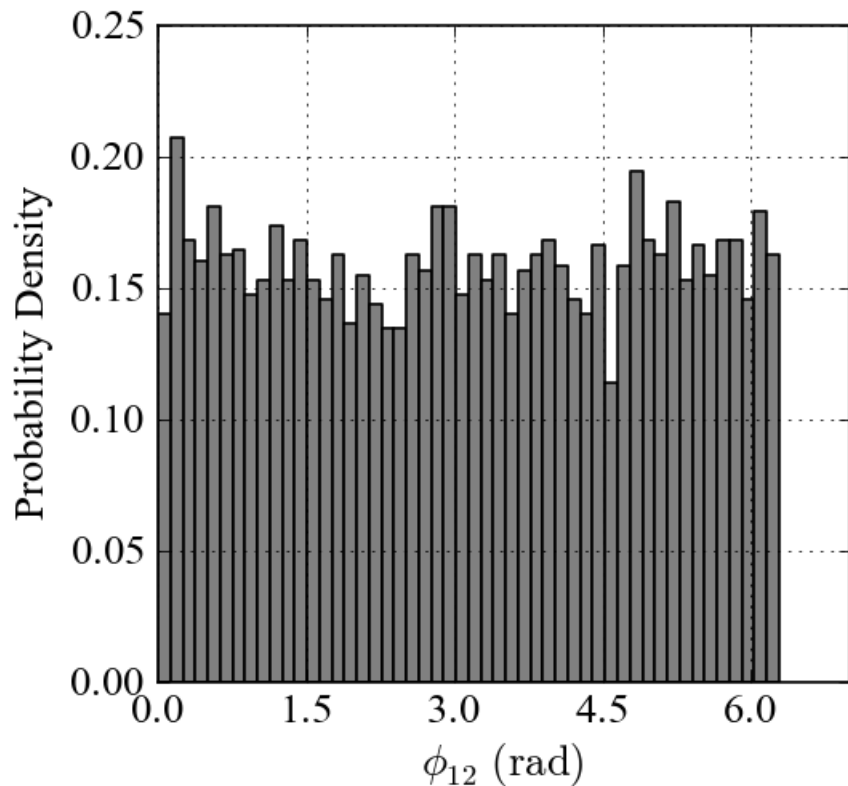
- ▣ 1) Both aligned
- ▣ 2) Dynamically formed, isotropic distribution – remains isotropic
- ▣ 3) Both BHs aligned prior to the second supernova – equally misaligned afterwards - freely precess
- ▣ 4) Secondary aligned prior to the second supernova via tides, primary misaligned (as in Gerosa et al 2013)

# Results in terms of these weird angles

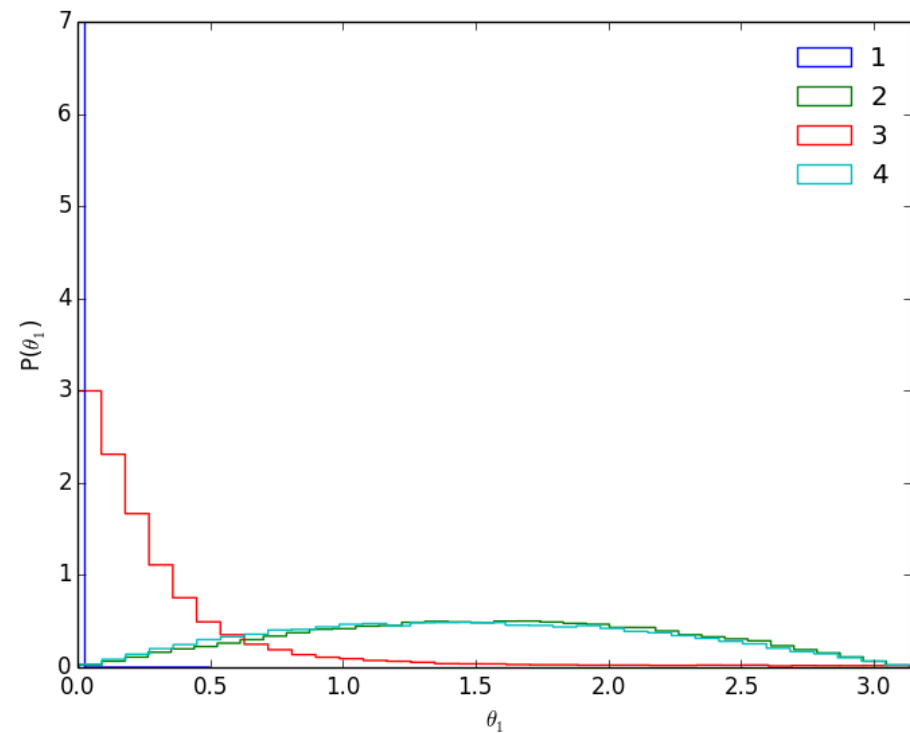
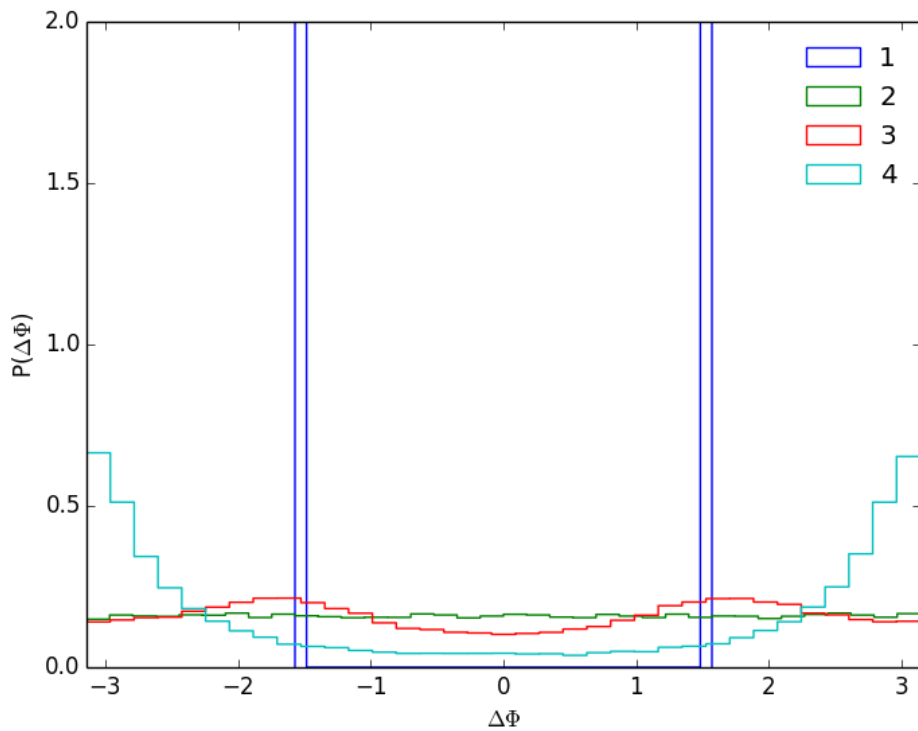


# What we might actually measure (1)

- Parameter estimation using LALINFERENCE\_MCMC
- Inject and recover using PhenomP waveform model



# What we might actually measure (2)



# Double pulsar – messes this up

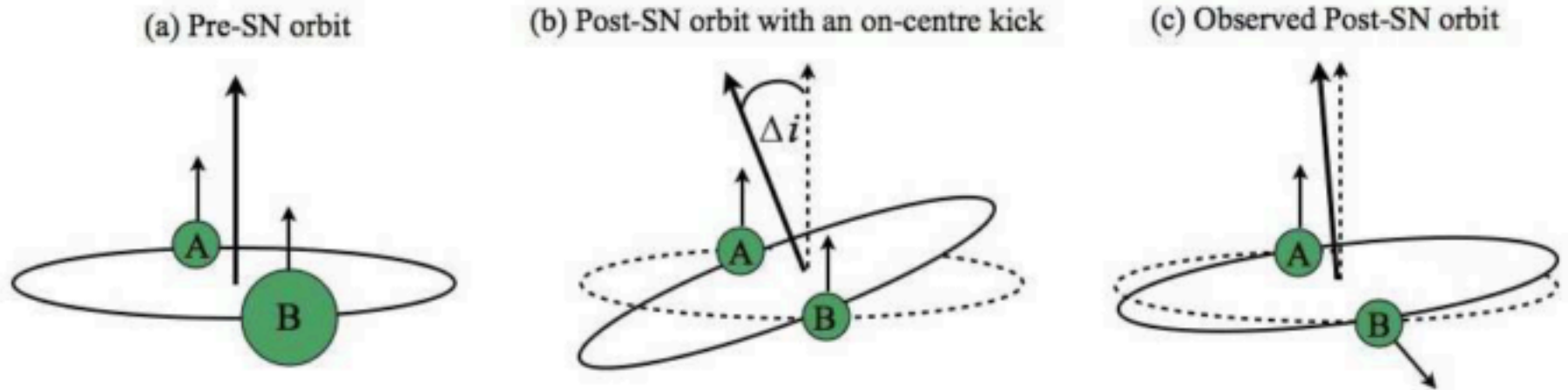


Fig. 1.— Effect of SN kick on binary orbit. The pre-SN orbit containing pulsar A and pulsar B's progenitor is shown in (a). The effect of an on-center SN kick that slightly changes the inclination of the orbit is illustrated in (b). Notice the post-SN alignment of the two pulsars' spin axes. Part (c) illustrates the present-day orbit with a 130 degree misalignment between pulsar B's spin axis and the orbital axis.

Farr et al 2011

# Conclusions/Future work

- In general, spins in BBH may not be aligned with the orbital angular momentum following a second supernova, leading to precession of the spins
- Spin-orbit resonances are effective in BBH systems with unequal misalignment angles, which may be true for astrophysically formed compact binaries
- Resonances binaries are attracted to depends on the formation mechanism of the binary
- Looking for clustering in these angles therefore can tell you about the compact binary channels
- Runs currently ongoing – wish me luck!
- Include some more physics, do some more work